

MGTbind: a comprehensive database of molecular glue ternary interactome

Jintao Zhu^{1,†}, Yiyao Liao^{2,†}, Haoyu Lin^{1,†}, Juan Xie³, Zhichao Deng⁴, Jinyu Han⁵, Zhen Zhang⁵, Jinchuan Xiao⁵, Zhiyao Wang³, Shuaipeng Zhang⁵, Luhua Lai^{1,3,6,7,*}, Jianfeng Pei^{1,*}

¹Center for Quantitative Biology, Academy for Advanced Interdisciplinary Studies, Peking University, Beijing 100871, China

²School of Life Sciences, Peking University, Beijing 100871, China

³BNLMS, College of Chemistry and Molecular Engineering, Peking University, Beijing 100871, China

⁴School of Pharmaceutical Sciences, Peking University, Beijing 100191, China

⁵Infinite Intelligence Pharma, Beijing 100083, China

⁶Peking-Tsinghua Center for Life Sciences, Academy for Advanced Interdisciplinary Studies, Peking University, Beijing 100871, China

⁷Peking University Chengdu Academy for Advanced Interdisciplinary Biotechnologies, Chengdu, Sichuan 610213, China

*To whom correspondence should be addressed. Email: jfpei@pku.edu.cn

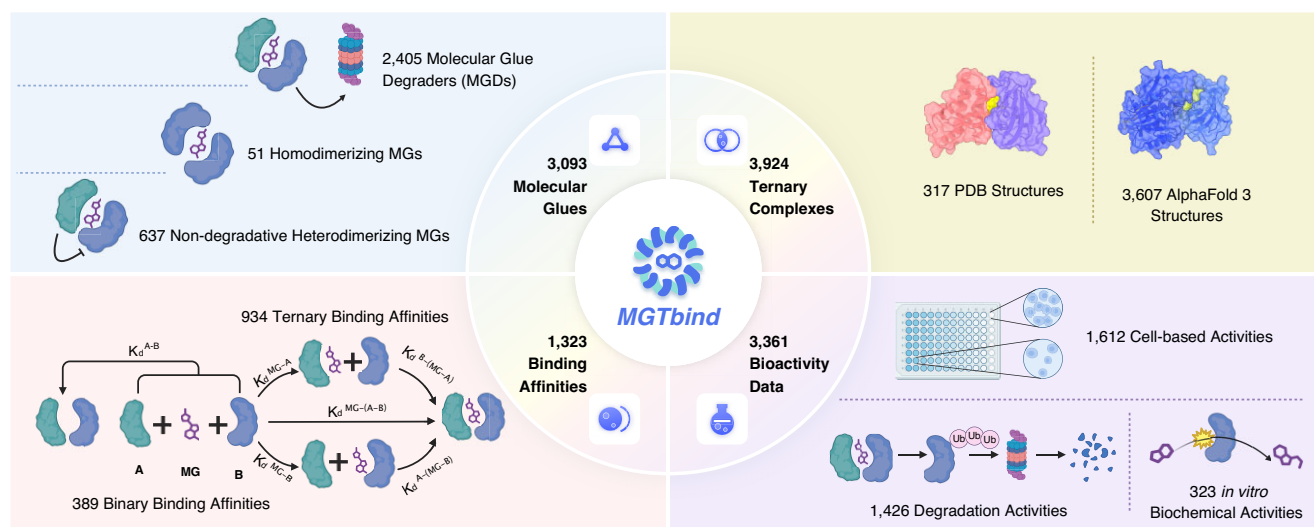
Correspondence may also be addressed to Luhua Lai. Email: lhilai@pku.edu.cn

[†]The first three authors should be regarded as Joint First Authors.

Abstract

Molecular glues (MGs) are an emerging class of small molecules capable of inducing or enhancing protein–protein interactions, leading to reprogramming of cellular events. In recent years, MG discovery has gained significant attention in drug discovery and synthetic biology studies. However, MG discovery remains exceptionally challenging as it continues to rely on serendipity and experimental screening efforts. In order to contribute data resources to facilitate the rational design of MGs, we developed the molecular glue and ternary binding (MGTbind) database, providing comprehensive resources about ternary structures and experimental data for the coverage of MG-engaged interactome. MGTbind database contains 3093 manually curated MGs with their chemical structures and physicochemical properties, along with 3924 ternary interactions with bioactivity measurements (e.g. degradation capacities for MG degraders, *in vitro* biochemical activities and cellular activities). Hierarchical binding affinity is also collected to enable exploring of cooperative binding mechanisms. Ternary complex structural data are systematically integrated, either from the Protein Data Bank or generated by AlphaFold 3. All of them can be intuitively analyzed and visualized along with various predicted metrics. A fully functional and user-friendly web interface that allows global search and smooth browsing is provided and is freely accessible at <https://mgtbind.pkumdl.cn>.

Graphical abstract



Received: August 11, 2025. Revised: September 12, 2025. Accepted: September 29, 2025

© The Author(s) 2025. Published by Oxford University Press.

This is an Open Access article distributed under the terms of the Creative Commons Attribution-NonCommercial License

(<https://creativecommons.org/licenses/by-nc/4.0/>), which permits non-commercial re-use, distribution, and reproduction in any medium, provided the

original work is properly cited. For commercial re-use, please contact reprints@oup.com for reprints and translation rights for reprints. All other

permissions can be obtained through our RightsLink service via the Permissions link on the article page on our site—for further information please contact journals.permissions@oup.com.

Introduction

Molecular glues (MGs), an emerging class of chemoproteomic proximity-inducing agents, are small molecules capable of altering protein–protein interactions (PPIs), either through inducing neomorphic PPIs or stabilizing native ones [1–4]. MGs present a transformative proximity-based strategy in drug discovery, significantly expanding the target space to previously “undruggable” proteins [5–8]. Over 15 FDA-approved drugs, though not intentionally discovered as MG, have hundreds of clinical applications and have treated millions of patients for decades [5]. Mechanistically, engagement of MG can induce a neosurface on one protein, enabling the recruitment of a second protein partner [9–11]. The formation of ternary complex selectively rewires cellular interactomes, ultimately modulating protein functions, such as modification, stability, and degradation [10–12]. Beyond therapeutic usage, MGs also serve as valuable tools in synthetic biology for engineering chemically inducible systems to precisely control cellular signaling [13–17].

A considerable number of MGs have been identified toward a wide variety of PPIs, such as KRAS(G12C)-CYPA [18, 19], CRBN with its neosubstrate space [20, 21], and 14-3-3 hub protein with client partners [22]. Based on their mechanisms of action (MOA) and downstream effects, MGs comprise three major categories: MG degraders (MGDs), non-degradative heterodimerizing MGs, and homodimerizing MGs [23]. MGDs are modulators in targeted protein degradation, and typically exert functions by inducing PPIs between E3 ligase and neosubstrates for proteasomal degradation [10, 24]. Compared to bifunctional PROTACs, MGDs exhibit better drug-like properties [25]. Currently, there have been notable clinical development for MGDs, with over a dozen more in clinical trials [26, 27]. As non-degradative alternatives, heterodimerizing MGs expand to a wider range of heterologous interactomes [28], while homodimerizing MGs induce self-association of target proteins [23]. Although a few public databases collect some MGs, such as ChEMBL [29], PubChem [30], and DrugBank [31], no dedicated database is available and particularly structured resources are quite limited.

Despite substantial progress, the discovery of MGs has relied largely on serendipity and experimental screening efforts, and the rational design remains exceptionally challenging [25]. MGs exhibit high cooperativity [32], which favors the formation of ternary complexes despite low or undetectable binding affinity toward any two components [33]. The unique binding mechanism usually involves conformational changes in the participating proteins, leading to the remodeling of surface physicochemical properties and reshaping [9, 34]. It is crucial to map the MG chemical space to fully understand which small molecules can mediate such mechanism. Furthermore, chemically induced PPIs deviate from natural evolutionary traces, and are biophysically driven [35]. Unfortunately, deeper structural insights and binding pattern understanding are hindered by the lack of extensive coverage of MG-engaged interactome.

To address these gaps, we developed MGTbind, a molecular glue and ternary binding database for the coverage of MG-engaged interactome. MGTbind provides carefully curated and standardized data on explored chemical space of MGs, ternary interactome, and experimentally measured activity data manually extracted from scientific literature and patents. MGTbind comprises not only MGDs mediated by a

diverse array of E3 ligases, but also non-degradative MGs, documenting a broad spectrum of gluable PPIs. To further advance the structural insights, MGTbind uniquely provides either experimentally determined ternary structures or predicted structures by AlphaFold 3 (AF3) [36] for every interaction. At present, MGTbind represents a comprehensive resource that, to our knowledge, has not been systematically integrated in existing databases. It aims to facilitate rational design of MGs especially in a structure-based manner, and provide a readily accessible platform to investigate the chemically regulated landscape of cellular PPIs.

Materials and methods

Data collection

The data collection workflow of MGTbind is illustrated in Fig. 1. The information of MGs was manually collected from scientific literatures and patents. Specifically, the PubMed database and Google Patent were searched using the keywords of “molecular glue”, “MG degrader”, “PPI stabilization”, “ternary complex”, and “chemically induced proximity”. Next, the search results were carefully and manually inspected and the irrelevant ones were ruled out. For each identified MG, the chemical structure was obtained by the optical chemical structure recognition tool MolMiner [37] with human inspection, and a brief introduction was summarized based the factual content from publications. The collected MGs were classified as heterodimerization-nondegrader, homodimerization, and heterodimerization-degrader based on the description in the corresponding literatures.

The information of MG-engaged PPIs was also extracted, including interacting mode types (domain–domain or domain-motif) [38], MOA types, involved protein names, UniProt IDs, and protein sequences with the annotations of mutation site and phosphorylation site. For covalent MGs, the covalent reaction and specific residue to form the covalent bond were annotated. As ternary structures play an important role in structure-based MG design, we specifically collected the experimentally solved structures from the Protein Data Bank (PDB) [39], along with PDB IDs and structure determination methods. For those without available experimental structures, AF3 was used to generate five top-ranked MG ternary complex structures with default settings and five random seeds. Our recent benchmarking study demonstrated that AF3 performed best among all tested co-folding methods (including Boltz-1, Chai-1, Protenix, and RoseTTAFold All-Atom), achieving 50.6% success rate in PPI prediction and 32.9% in MG-protein interaction recovery [40].

To enable possible cooperative binding mechanism and structure-activity relationship (SAR) studies, the binding affinity and various bioactivity data were also incorporated to the database. It is noteworthy that binding affinity data have been compiled for both binary interactions within ternary systems and complete ternary complexes. As for bioactivity data, MGTbind curated degradation capacities, *in vitro* biochemical activities and cellular activities with experimental descriptions and measurements. The degradation capacities were tailored for MGDs, and consisted of the half-maximal degradation concentration (DC_{50}) with the cell line annotation, the maximal level of protein degradation (D_{max}), and the percentage degradation at a certain concentration.

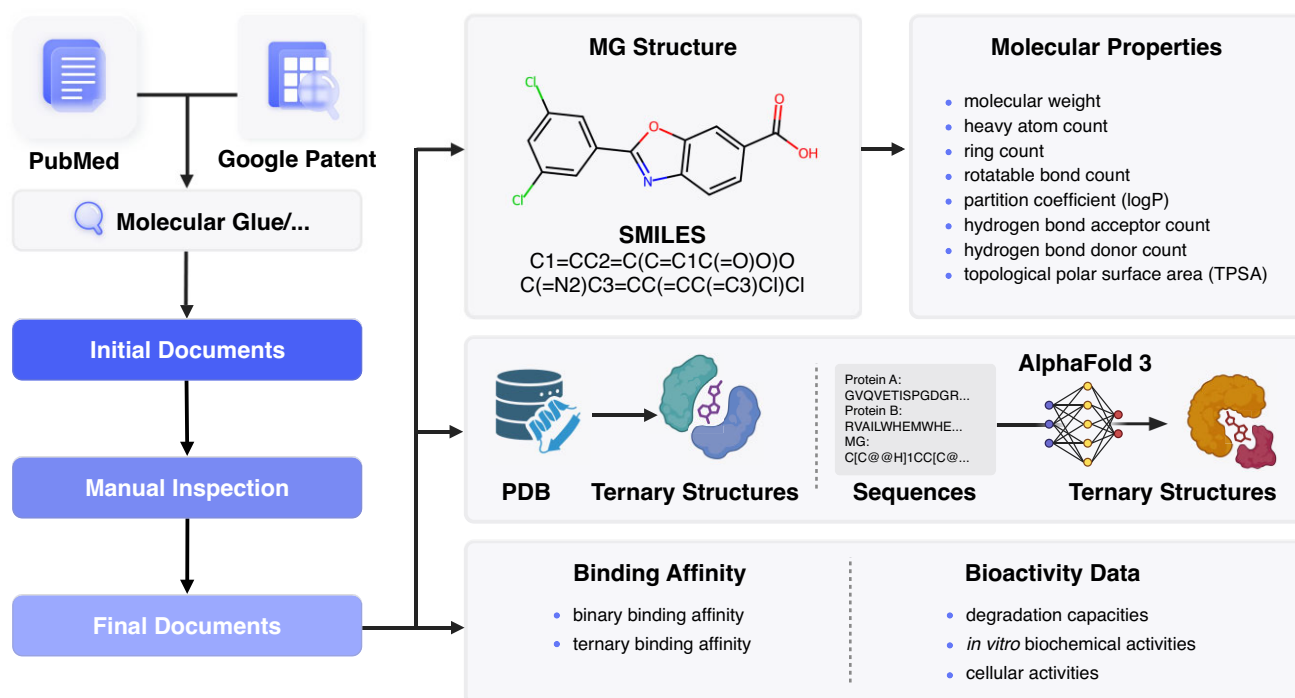


Figure 1. An illustration of the basic data collection workflow.

Data processing

The MGs in MGTbind were annotated with molecular formula, canonical SMILES, InChI and InChIKey representations from RDKit (<http://www.rdkit.org>). The IUPAC name was generated by RDKit and STOUT [41]. In addition, eight key physicochemical properties related to drug-likeness were calculated by RDKit, including molecular weight, heavy atom count, ring count, rotatable bond count, partition coefficient (logP), hydrogen bond acceptor count, hydrogen bond donor count, and topological polar surface area. To provide more authoritative information, MGs were mapped into the ChEMBL [29] and PubChem [30] where applicable. 2048-bit Morgan fingerprints with a radius of 2 were also generated by FPsSim2 (<https://github.com/chembl/FPSim2>) to enable molecular similarity-based retrieval function.

All curated ternary structures were preprocessed using the Protein Preparation Wizard module [42] of Schrödinger Release 2021-2, including assigning bond orders, adding hydrogens, creating disulfide bonds, filling in missing side chains, assigning protonation state, optimizing hydrogen bond network, and minimizing hydrogen atoms with the OPLS_2005 force field. The interactions between MGs and PPI interfaces were further analyzed using ProLIF [43], and were exported for online interactive visualization.

To evaluate the quality of AF3-predicted MG-protein structures, we introduced two confidence metrics (see details in the [Supplementary Data](#)): “MG Chain ipTM”, which serves as a reliable indicator of the average confidence level for the interface between the MG and other protein chains, and “Avg. pLDDT of MG”, which represents the mean pLDDT value across all heavy atoms of MG. Based on our previous evaluation results [40], we conducted an acceptance criterion test experiment as described in the [Supplementary Data](#). The results suggest that an “MG Chain ipTM” value >0.68 combined with an “Avg. pLDDT of MG” value above 70 serves as

an effective acceptance criterion for AF3-predicted structures, achieving an F1 score of 0.71, with a precision of 0.58 and a recall of 0.93.

MGTbind website implementation

MGTbind adopts a separation of front-end and back-end architecture. The front-end was developed using the React framework (<https://react.dev>) and the Material UI component library (<https://mui.com>). The back-end was built with the lightweight Flask framework (<https://flask.palletsprojects.com>), and data were stored persistently in the PostgreSQL relational database (<https://www.postgresql.org>), which was mainly included in three tables: compounds, complexes, and citations. The Python back-end accesses the database through the SQLAlchemy ORM toolkit (<https://www.sqlalchemy.org>). The front-end embeds Mol* Viewer [44] for interactive 3D display of MG ternary complex structures and Ketcher (<https://lifescience.opensource.epam.com/ketcher>) for molecular structure editing. Furthermore, the Ketcher editor supports three structure-based search options: exact structure match, substructure match, and similar structure search. The interactive 2D interactions between MGs and proteins are displayed using vis.js (<https://visjs.org>). Other interactive charts in MGTbind are created with Chart.js (<https://www.chartjs.org>) or Plotly.js (<https://plotly.com/javascript>).

Results

Database content

The current release of MGTbind contains 3093 MGs, which are classified into 2405 MGDs, 637 non-degradative heterodimerizing MGs, and 51 homodimerizing MGs (Fig. 2A). According to our molecular property analysis, 60% of MGs meet Lipinski’s “Rule of 5” [45] (Fig. 2B–G). Out of 3924

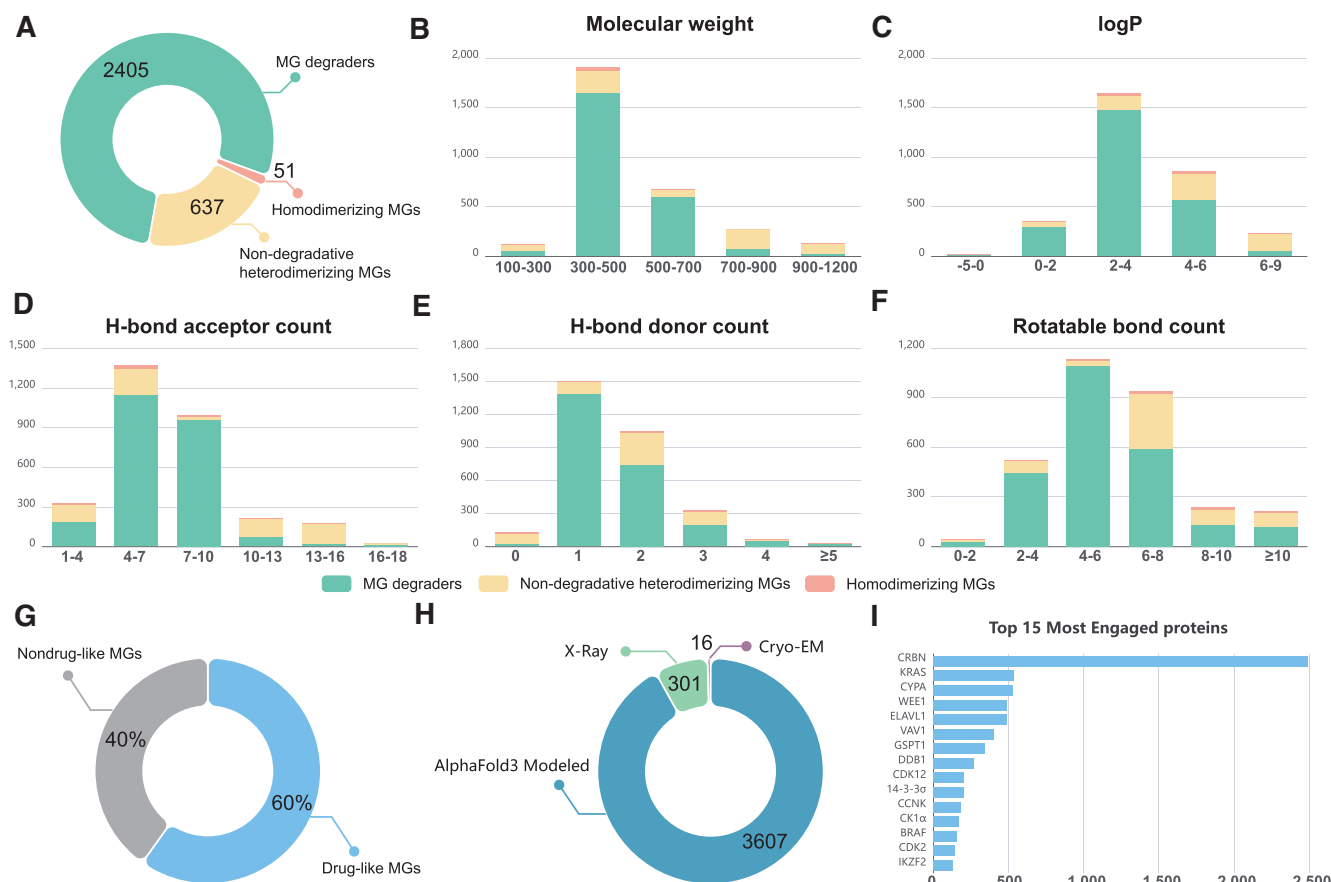


Figure 2. Data statistics of MGTbind. (A) Number of three types of MGs. The molecular property distributions for molecular weight (B), logP (C), hydrogen bond acceptor count (D), hydrogen bond donor count (E), and rotatable bond count (F). Figure B–F share the same legend. (G) Proportion of drug-like MGs satisfying Lipinski's "Rule of 5". (H) Number of three structure determination methods. (I) The top-15 frequent proteins engaged in MG ternary interactions.

ternary interactions, a total of 2891 are involved in MGD-induced degradation via E3 ligases. The remaining complexes consist of 979 heterodimerizing and 54 homodimerizing complexes. To provide a deeper structural understanding, MGTbind integrates 317 experimentally determined ternary structures from PDB (301 crystal structures and 16 cryo-EM structures) and 3607 AF3-generated ternary complex structures (Fig. 2H). Among these, 211 structures are covalently bound by a MG. The MG interactome covers 180 unique PPIs across 211 proteins. The top-15 frequent proteins engaged in MG ternary interactions are shown in Fig. 2I. Furthermore, various types of activity data are collected, including 389 binary binding affinity records, 934 ternary binding affinity records, 323 *in vitro* biochemical activity records, 1612 cell-based activity records, and 1426 degradation activity records (specific to the MGDs). All MG data, ternary interactions, literature collections, and PDB structures can be downloaded in the "Download" module of MGTbind website (<https://mgtbind.pkumdl.cn>).

The search engines in MGTbind

MGTbind provides search interfaces with multiple options for information retrieval. Quick search appears both in the middle of the website homepage and on the toolbar in the upper right corner throughout each page. The default option

searches against the MG compound database; MG ternary interactions can be searched when the "Complex Database" option is selected on the top of the search box or the toggle switch is activated (the black indicator turn left) for the basic search on the toolbar.

To search for MGs, both the text-based and structure-based query are supported. Text-based search allows users to simply enter any term of interest and press the "Search" button to explore the MG compound database (Fig. 3A). By default, the search is performed on all fields, but users can specify optional fields in the drop-down box on the left of the search box. The optional fields include three distinct types: character type (e.g. MG ID, name, different molecular representations, PubChem ID, ChEMBL ID), option type (e.g. MOA type, binding type), and numerical range type (e.g. eight physicochemical properties). In addition, a powerful advanced search allows users to specify any number of query terms and combine them with the Boolean operators (AND/OR/NOT) to broaden or refine a search. It is worth noting that the fields of character type use an implicit AND operator when users enter two or more whitespace-separated terms. For example, typing abscisic acid is equivalent to typing abscisic AND acid. However, enclosing a query in quotation marks disables the implied-AND logic, and will instead be treated as a single search term. For the structure-based search engine, users can paste a SMILES string, upload a SDF file or sketch a molecule

A Compound Database Search

Search in: Compound Database

Find: Name LYG

AND Type heterodimerization-degrader

AND Exact Mass Min: 100.00 Max: 500

Example 1: Search all fields for RMC-7977

Example 2: Search by compound name

Example 3: Search by SMILES string

33 Compounds Results for "name:LYG type:heterodimerization-degrader exact_mass:>=100 exact_mass:<=500"

B Structure-Based Search

Structure Search

Match Method: Exact Structure, Substructure, Similar Structure

Similarity Threshold: 0.5

21 Compounds Results for "similar_structure:C1=CC=C2N=NN(C3CCC(=O)NC3=O)C(=O)C2=C1:0.5"

C Complex Database Search

Search in: Complex Database

Find: All Fields BRD4

AND MOA Type heterodimerization-degradative

Example 1: Search all fields for UniProt ID

Example 2: Search by protein and MOA type

Example 3: Search by protein pair

30 Complexes Results for "All:BRD4 moa_type:heterodimerization-degradative"

Figure 3. Data query in MGTbind. (A) Text-based search for MG information. Here, a search example for LYG series MG degraders with a molecular weight <500 is shown. (B) Structure-based MG search within a Ketcher editor. A molecular query and search result cards are shown based on fingerprint similarity with a threshold of 0.5. (C) Text-based search for MG ternary complex information. A query example and search result cards of degradative ternary interactions where BRD4 is involved.

via the Ketcher editor (Fig. 3B). After the query molecule has been imported, one of the three searching options (exact structure/substructure/similar structure) can be chosen. In the similar structure search option, the Morgan fingerprint will be generated for the query molecule and Tanimoto similarities will be computed against the compound database in MGTbind. The search results are a list of hit cards with several indicative information (e.g. MG ID, MG name, MOA type) as well as the similarity score for the similarity-based structure search, and can be downloaded via the “Export” button.

To search for ternary complexes, the text-based query is supported (Fig. 3C). The ternary complex search engine shares the same mechanism with text-based MG search engine. However, the searchable fields including two types: character type (e.g. complex ID, protein A/B, PDB ID, experimental assays) and option type (e.g. MOA type, domain type, binding type, structure determination method). Among them, protein A/B field allows users to access the query protein-involved ternary interactions by its protein name, gene name, or UniProt ID.

Data browsing of database

In order to help users to explore the information of interest more efficiently, MGTbind provides three intuitive browse interfaces: “Compounds Browse”, “Complexes Browse”, and “Citations Browse”. “Compounds Browse” will display the list of all MGs with the columns of MG ID, name, MOA type, PubChem ID, ChEMBL ID, Binding Type, different molecular representations and citations (Fig. 4). Similarly, “Complexes Browse” allows users to retrieve all MG ternary interactions and their structure determination methods. For AF3-generated structures, three indication columns for the modeling quality estimation are introduced: a global quality metric, “Ranking Score”, and two local metrics for the MG-binding interface quality, “MG Chain ipTM” and “Avg. pLDDT of MG”. Moreover, users can access all collected documents in MGTbind and trace the scientific evidence of MG and ternary interactions in more detail by “Citations Browse”.

These browsable interfaces offer a high degree of customizability through its column management feature, allowing users to selectively display or hide specific data fields,

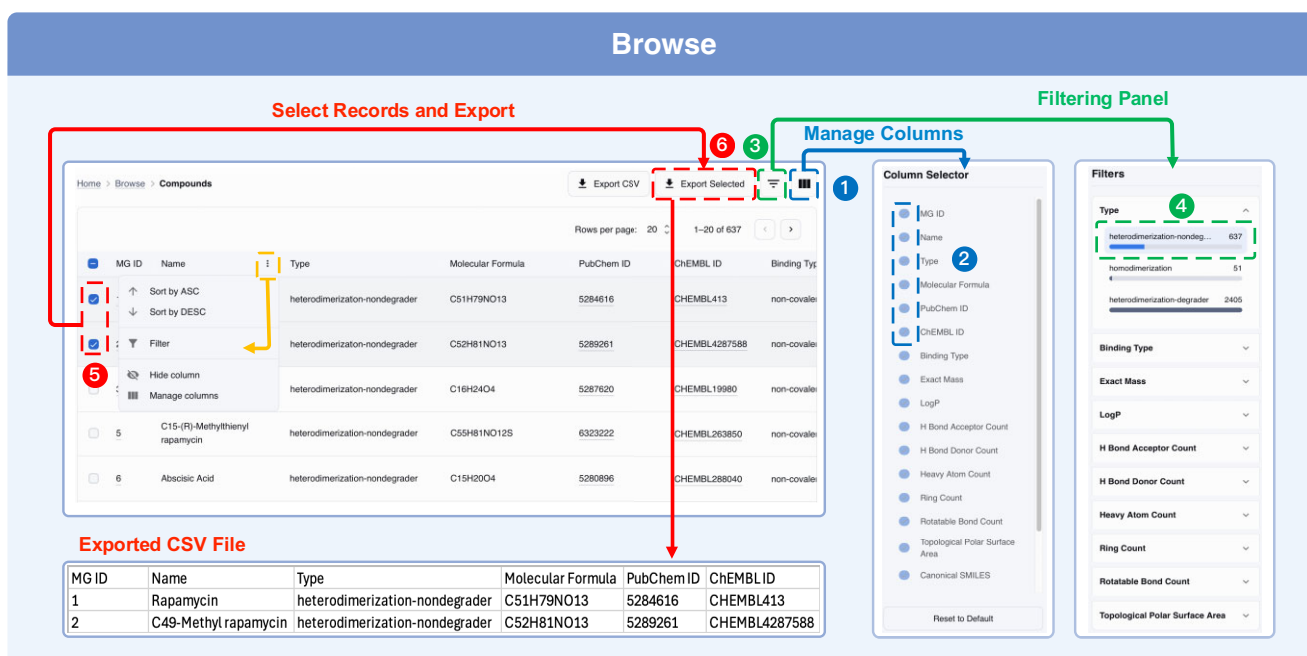


Figure 4. The “Compounds Browse” in MGTbind, with the functions of columns management, filtering, manual selection, and data download.

thereby focusing on information of particular interest. To facilitate precise data queries, filtering tools are also integrated, which enable users to set conditions to quickly locate information of interest. Furthermore, the interfaces support a manual selection function, where users can tag specific rows for inclusion in a built-in data download feature. This allows the selected data to be exported into a csv format file, facilitating offline analysis and further research. Together, these features provide users with a powerful and flexible platform to customize their browse and analysis of the MG data within MGTbind.

The detailed information of MGs

The detailed information of a MG is organized into a MG summary page. If users are interested in a MG, its detailed information can be accessed by clicking on the “View Compound Details” button at the searched result card or clicking on its MG ID at the datasheet in “Compounds Browse”. In a MG summary page, five tabs are incorporated, including structure, brief introduction, compound details, associated complexes, and associated citations. The structure tab displays 2D structure depiction drawn by RDKit; the brief introduction tab describes factual content from relevant literature; the compound details tab contains MOA type, eight calculated properties, five molecular representations, PubChem ID, and ChEMBL ID; the associated complexes tab contains a browsable ternary complex table of its interactome, and allows internal linking to each summary page of its ternary complex; and the associated citations tab collects its relevant literature with PubMed ID and DOI.

The detailed information and display of MG-engaged ternary complex structures

To access a summary page of MG ternary complex, click on the “View Complex Details” button at the searched result card or click on its Complex ID at the datasheet in “Complexes

Browse”. Each summary page organizes information in the following modules: 3D structure visualization, protein-MG 2D interaction display, predicted metrics summary and visualization, ternary complex information, experimental data, and associated citations. These modules are arranged from top to bottom on the page.

The 3D structure visualization module embeds Mol* Viewer to display both PDB structures and AF3-generated structures, which provides valuable information to the structure-based design of MG-mediated PPI.

For a ternary complex with an available PDB structure, the raw PDB structure is displayed by default, with the entire structure colored by chain (Fig. 5A). On the top of the Mol* panel, a selectable box provides an option to access and display the processed structures. An expandable “Sequence” panel is positioned in the middle of the panel, presenting the protein sequence and identifier information for small molecules (MG is included). “Download” buttons in the bottom right corner and the selectable box allow users to download the structure coordinate files. The processed structures are analyzed with ProLIF to identify interactions between each protein and the MG, and to generate 2D interaction diagrams (Fig. 5B). These interaction diagrams can be flexibly edited in an interactive visualization interface.

For the predicted ternary complex structure by AF3, MGTbind provides interactive molecular display for the top-5 structures ranked by the ranking score (Fig. 5C). The entire structure can be colored either by chain or by per-residue/atom pLDDT score. The MG can be zoomed in via single-clicking on the “Focus on MG” button, and then, its binding site within 5 Å around the MG and their interactions are shown as sticks and dashed lines, respectively. Additionally, when any two structures are selected, superimposed structures will be generated and displayed for analyzing structural distinctions.

To help users to assess the reliabilities of AF3-generated structures, the confidence measurements are summarized in the predicted metrics summary module (Fig. 5D), which

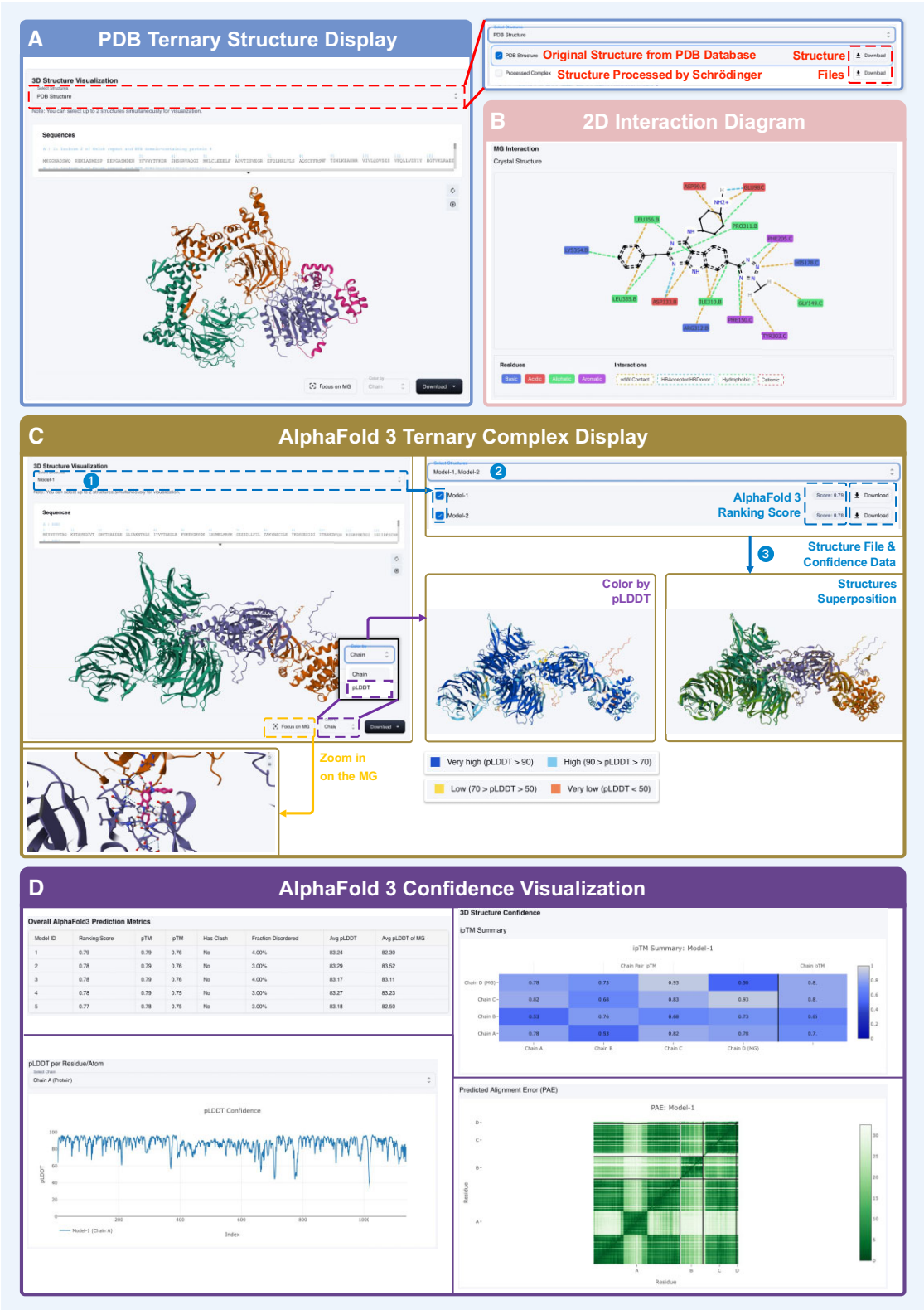


Figure 5. Ternary complex structure display and analysis in the summary page of MG ternary complex. **(A)** PDB structure display and **(B)** Protein-MG 2D interaction diagram of PDB ID 8VOJ. **(C)** AF3 structure display and pairwise superposition of MGTbind Complex ID 244. **(D)** The summary and visualization of AF3-predicted metrics of MGTbind Complex ID 244.

contains four tabs as described as following. The “Overall AlphaFold3 Prediction Metrics” tab provides a comprehensive summary table to display modeling metrics for the top-5 predicted structures, including Ranking Score, pTM, ipTM, Has Clash, Fraction Disordered, Avg. pLDDT, and Avg. pLDDT of MG. Additionally, the heatmap of Chain Pair ipTM and Chain ipTM is visualized in the “3D Structure Confidence” tab, which is useful to evaluate the MG binding interface quality. In the “pLDDT per Residue/Atom” tab, the pLDDT scores are plotted for each protein chain (residue level) and MG (atom level). Similarly, a PAE heatmap is visualized to gain insight into the reliability of relative position and orientations of different domains. These confidence data alongside structure coordinate CIF files are downloadable via the “Download” buttons (Fig. 5C).

The ternary complex information module provides access to the collected information of the MG-engaged PPI (see details in Fig. 6A). For a MGD, each protein is labeled as either an E3 ligase or a substrate. The basic information of the MG is also provided for checking MG structure and the MG summary page can be internally linked via the MG ID. To enable exploring of cooperative binding mechanisms, binary binding affinity, and ternary binding affinity data are provided (Fig. 6B). The experimental bioactivity data comprises molecular-level biochemical activities, cellular potency measurements, and protein degradation activities (specific to the MGDs) (Fig. 6C). Lastly, the associated citations module serves as an interface for users to find out more detailed information about the ternary interaction (Fig. 6D).

Conclusion and perspectives

MGs are important chemically induced proximity entities and open broad applications in biotechnology ranging from drug discovery to synthetic biology. However, rational MG design remains a great challenge, primarily due to no specialized database available to supply comprehensive information of MGs and their interactomes. Therefore, we present MGTbind, a comprehensive database of MGs and ternary structures. The distinct merits of MGTbind can be summarized as: (i) it has a high coverage of MGs with different types; (ii) it provides a comprehensive interactome platform with massive ternary structures, which is highly useful for structure-based MG design; and (iii) it contains multi-scale activity data for cooperative binding mechanisms and cellular responses. We believe that both wet-lab and *in silico* researchers would greatly benefit from these resources. Medicinal chemists can efficiently search for a specific PPI and easily access target-specific MGs to support SAR study and structural optimization. Computational chemists can leverage the well-curated chemical space of MGs to develop scoring functions for glue-like molecules. The ternary complex structures in MGTbind enable structure-based virtual screening and *de novo* molecular generation to identify novel MG scaffolds. Importantly, these structural data will facilitate the development and benchmarking of advanced computational models, including predictions of MG ternary complexes, ternary interaction profiling, and free energy calculations.

As the rapid accumulation of MG knowledge, we will continue to update MGTbind regularly to provide more extensive data and knowledge, and improve the functions of the web interface. Despite the breadth of the current database, it pri-

marily encompasses MGs that act at the immediate protein-protein interface. We recognize several important and emerging gaps in the current coverage, such as the recently reported class of allosteric or distal-induction MGs [46], which operate remotely from the binding interface. Furthermore, the landscape of chemically induced proximity is expanding to include glues for biomolecules beyond proteins, such as those stabilizing protein-nucleic acid complexes [47–49]. The inclusion of these novel modalities represents a key direction for the future development of MGTbind. A data submission feature will be added to allow users to upload newly discovered MG ternary interactions to the database. Protein sequence- and structure-based search engines will also be implemented. Additionally, while MGTbind provides comprehensive structural data, AF3-predicted structures are currently dominant, and their accuracy inherently depends on predictive power of AF3. There remains room to improve the quality of modeled structures. Future advances in AI co-folding models will be pivotal to addressing this limitation. We expect that MGTbind, as a dedicated and well-organized MG related data resource, will provide substantial value to the rising field of rational MG design.

Acknowledgements

We thank Yibo Li from the College of Chemistry and Molecular Engineering, Peking University for providing server infrastructure for the backend. We gratefully acknowledge Google DeepMind and Isomorphic Labs for open-sourcing AF3 and enabling academic access to its model parameters. Our work utilizes valuable structural resources generated by AF3, in compliance with the AF3 Output Terms of Use.

Author contributions: Jintao Zhu (Conceptualization [equal], Data curation [equal], Formal analysis [equal], Investigation [equal], Methodology [equal], Project administration [equal], Resources [equal], Validation [equal], Visualization [equal], Writing—original draft [lead], Writing—review & editing [equal]), Yiyao Liao (Data curation [equal], Formal analysis [equal], Investigation [equal], Resources [equal], Validation [equal], Visualization [equal]), Haoyu Lin (Investigation [equal], Methodology [equal], Resources [equal], Software [lead], Validation [equal], Writing—review & editing [supporting]), Juan Xie (Data curation [supporting], Formal analysis [equal], Investigation [equal], Validation [equal], Writing—review & editing [supporting]), Zhichao Deng (Methodology [supporting], Validation [supporting]), Jinyu Han (Methodology [equal]), Zhen Zhang (Visualization [equal]), Jinchuan Xiao (Methodology [supporting]), Zhiyao Wang (Data curation [supporting]), Shuaipeng Zhang (Software [supporting]), Luhua Lai (Funding acquisition [equal], Supervision [equal], Writing—review & editing [lead]), and Jianfeng Pei (Conceptualization [equal], Funding acquisition [lead], Project administration [equal], Supervision [equal], Writing—review & editing [lead]).

Supplementary data

Supplementary data is available at NAR online.

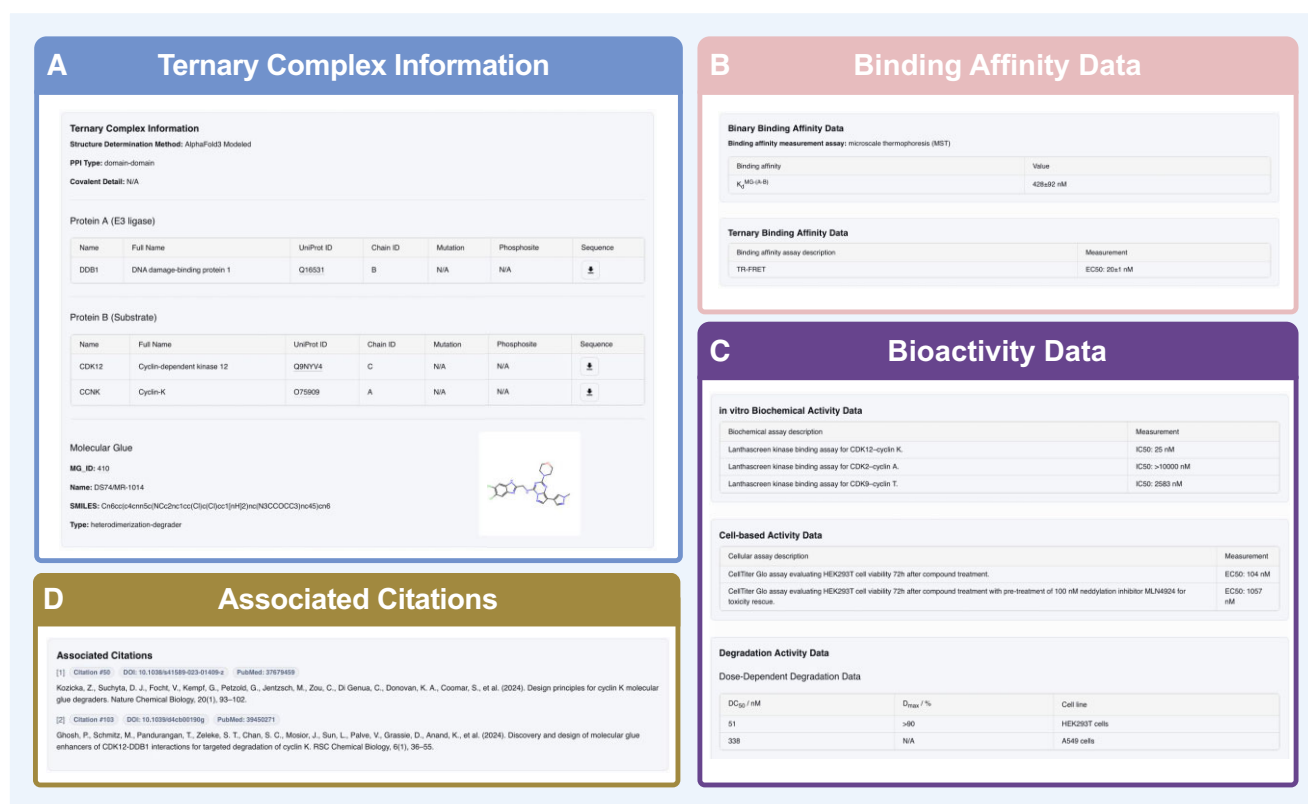


Figure 6. The ternary complex information and experimental data for MGTbind Complex ID 520. **(A)** Ternary complex information, **(B)** binding affinity data, **(C)** bioactivity data, and **(D)** associated citations tabs in the summary page of MG ternary complex.

Conflict of interest

J.H., Z.Z., J.X., and S.Z. are current employees of Infinite Intelligence Pharmaceutical Technology Co., Ltd.

Funding

National Natural Science Foundation of China [22033001, T2321001]; Major Project of Guangzhou National Laboratory [GZNL2024A01005]; National Key R&D Program of China [2023YFF1205103]; Chinese Academy of Medical Sciences [2021-I2M-5-014]; Anhui's Plans for Major Provincial Science&Technology Projects [202303a07020009]; Beijing Natural Science Foundation [QY25135]. Funding to pay the Open Access publication charges for this article was provided by National Natural Science Foundation of China [22033001].

Data availability

MGTbind v1.0 was launched on 18 July 2025. The website is freely accessible to all users without any login requirement at <https://mgtbind.pkumdl.cn>.

References

- Schreiber SL. The rise of molecular glues. *Cell* 2021;184:3–9. <https://doi.org/10.1016/j.cell.2020.12.020>
- Stanton BZ, Chory EJ, Crabtree GR. Chemically induced proximity in biology and medicine. *Science* 2018;359:eaao5902. <https://doi.org/10.1126/science.aao5902>
- Garber K. The glue degraders. *Nat Biotechnol* 2024;42:546–50. <https://doi.org/10.1038/s41587-024-02164-9>
- Zhu J, Lai L, Pei J. Toward *in silico* design of protein-protein interaction stabilizers. *ACS Cent Sci* 2023;9:861–3. <https://doi.org/10.1021/acscentsci.3c00545>
- Dewey JA, Delalande C, Azizi SA *et al*. Molecular glue discovery: current and future approaches. *J Med Chem* 2023;66:9278–96. <https://doi.org/10.1021/acs.jmedchem.3c00449>
- Hanzl A, Inghelram C, Schmitt S *et al*. Primed for degradation: how weak protein interactions enable molecular glue degraders. *Curr Opin Struct Biol* 2025;92:103052. <https://doi.org/10.1016/j.sbi.2025.103052>
- Hinterdorfer M, Spiteri VA, Ciulli A *et al*. Targeted protein degradation for cancer therapy. *Nat Rev Cancer* 2025;25:493–516. <https://doi.org/10.1038/s41568-025-00817-8>
- Chirnomas D, Hornberger KR, Crews CM. Protein degraders enter the clinic—a new approach to cancer therapy. *Nat Rev Clin Oncol* 2023;20:265–78. <https://doi.org/10.1038/s41571-023-00736-3>
- Watson ER, Novick S, Matyskiela ME *et al*. Molecular glue CELMoD compounds are regulators of cereblon conformation. *Science* 2022;378:549–53. <https://doi.org/10.1126/science.add7574>
- Schreiber SL. Molecular glues and bifunctional compounds: therapeutic modalities based on induced proximity. *Cell Chem Biol* 2024;31:1050–63. <https://doi.org/10.1016/j.chembiol.2024.05.004>
- Robinson SA, Co JA, Banik SM. Molecular glues and induced proximity: an evolution of tools and discovery. *Cell Chem Biol* 2024;31:1089–100. <https://doi.org/10.1016/j.chembiol.2024.04.001>
- Gerry CJ, Schreiber SL. Unifying principles of bifunctional, proximity-inducing small molecules. *Nat Chem Biol* 2020;16:369–78. <https://doi.org/10.1038/s41589-020-0469-1>

13. Spencer DM, Wandless TJ, Schreiber SL *et al.* Controlling signal transduction with synthetic ligands. *Science* 1993;262:1019–24. <https://doi.org/10.1126/science.7694365>
14. Glasgow AA, Huang YM, Mandell DJ *et al.* Computational design of a modular protein sense-response system. *Science* 2019;366:1024–8. <https://doi.org/10.1126/science.aax8780>
15. Foight GW, Wang Z, Wei CT *et al.* Multi-input chemical control of protein dimerization for programming graded cellular responses. *Nat Biotechnol* 2019;37:1209–16. <https://doi.org/10.1038/s41587-019-0242-8>
16. Giordano-Attianese G, Gainza P, Gray-Gaillard E *et al.* A computationally designed chimeric antigen receptor provides a small-molecule safety switch for T-cell therapy. *Nat Biotechnol* 2020;38:426–32. <https://doi.org/10.1038/s41587-019-0403-9>
17. Marchand A, Buckley S, Schneuing A *et al.* Targeting protein-ligand neosurfaces with a generalizable deep learning tool. *Nature* 2025;639:522–31. <https://doi.org/10.1038/s41586-024-08435-4>
18. Holderfield M, Lee BJ, Jiang J *et al.* Concurrent inhibition of oncogenic and wild-type RAS-GTP for cancer therapy. *Nature* 2024;629:919–26. <https://doi.org/10.1038/s41586-024-07205-6>
19. Schulze CJ, Seamon KJ, Zhao Y *et al.* Chemical remodeling of a cellular chaperone to target the active state of mutant KRAS. *Science* 2023;381:794–9. <https://doi.org/10.1126/science.adg9652>
20. Petzold G, Gainza P, Annunziato S *et al.* Mining the CRBN target space redefines rules for molecular glue-induced neosubstrate recognition. *Science* 2025;389:eadt6736. <https://doi.org/10.1126/science.adt6736>
21. Baek K, Metivier RJ, Roy Burman SS *et al.* Unveiling the hidden interactome of CRBN molecular glues. *Nat Commun* 2025;16:6831. <https://doi.org/10.1038/s41467-025-62099-w>
22. Tian Y, Li L, Wu L *et al.* Recent developments in 14-3-3 stabilizers for regulating protein-protein interactions: an update. *J Med Chem* 2025;68:2124–46. <https://doi.org/10.1021/acs.jmedchem.4c01936>
23. Konstantinidou M, Arkin MR. Molecular glues for protein–protein interactions: progressing toward a new dream. *Cell Chem Biol* 2024;31:1064–88. <https://doi.org/10.1016/j.chembiol.2024.04.002>
24. Oleinikovas V, Gainza P, Ryckmans T *et al.* From thalidomide to rational molecular glue design for targeted protein degradation. *Annu Rev Pharmacol Toxicol* 2024;64:291–312. <https://doi.org/10.1146/annurev-pharmtox-022123-104147>
25. Dong G, Ding Y, He S *et al.* Molecular glues for targeted protein degradation: from serendipity to rational discovery. *J Med Chem* 2021;64:10606–20. <https://doi.org/10.1021/acs.jmedchem.1c00895>
26. Tsai JM, Nowak RP, Ebert BL *et al.* Targeted protein degradation: from mechanisms to clinic. *Nat Rev Mol Cell Biol* 2024;25:740–57. <https://doi.org/10.1038/s41580-024-00729-9>
27. Sasso JM, Tenchov R, Wang D *et al.* Molecular glues: the adhesive connecting targeted protein degradation to the clinic. *Biochemistry* 2023;62:601–23. <https://doi.org/10.1021/acs.biochem.2c00245>
28. Repity ML, Deutscher RCE, Hausch F. Nondegradative synthetic molecular glues enter the clinic. *ChemMedChem* 2025;20:e202500048. <https://doi.org/10.1002/cmdc.202500048>
29. Zdrazil B, Felix E, Hunter F *et al.* The ChEMBL database in 2023: a drug discovery platform spanning multiple bioactivity data types and time periods. *Nucleic Acids Res* 2024;52:D1180–92. <https://doi.org/10.1093/nar/gkad1004>
30. Kim S, Chen J, Cheng T *et al.* PubChem 2025 update. *Nucleic Acids Res* 2025;53:D1516–25. <https://doi.org/10.1093/nar/gkae1059>
31. Knox C, Wilson M, Klinger CM *et al.* DrugBank 6.0: the DrugBank knowledgebase for 2024. *Nucleic Acids Res* 2024;52:D1265–75. <https://doi.org/10.1093/nar/gkad976>
32. Liu S, Tong B, Mason JW *et al.* Rational screening for cooperativity in small-molecule inducers of protein-protein associations. *J Am Chem Soc* 2023;145:23281–91. <https://doi.org/10.1021/jacs.3c08307>
33. Cao S, Kang S, Mao H *et al.* Defining molecular glues with a dual-nanobody cannabidiol sensor. *Nat Commun* 2022;13:815. <https://doi.org/10.1038/s41467-022-28507-1>
34. Kozicka Z, Thoma NH. Haven't got a glue: protein surface variation for the design of molecular glue degraders. *Cell Chem Biol* 2021;28:1032–47. <https://doi.org/10.1016/j.chembiol.2021.04.009>
35. Gainza P, Bunker RD, Townson SA *et al.* Machine learning to predict *de novo* protein–protein interactions. *Trends Biotechnol* 2025. <https://doi.org/10.1016/j.tibtech.2025.04.013>
36. Abramson J, Adler J, Dunger J *et al.* Accurate structure prediction of biomolecular interactions with AlphaFold 3. *Nature* 2024;630:493–500. <https://doi.org/10.1038/s41586-024-07487-w>
37. Xu Y, Xiao J, Chou C-H *et al.* MolMiner: you only look once for chemical structure recognition. *J Chem Inf Model* 2022;62:5321–8. <https://doi.org/10.1021/acs.jcim.2c00733>
38. Rui H, Ashton KS, Min J *et al.* Protein–protein interfaces in molecular glue-induced ternary complexes: classification, characterization, and prediction. *RSC Chem Biol* 2023;4:192–215. <https://doi.org/10.1039/D2CB00207H>
39. Burley SK, Bhatt R, Bhikadiya C *et al.* Updated resources for exploring experimentally-determined PDB structures and Computed Structure Models at the RCSB Protein Data Bank. *Nucleic Acids Res* 2025;53:D564–74. <https://doi.org/10.1093/nar/gkae1091>
40. Liao Y, Zhu J, Xie J *et al.* Benchmarking cofolding methods for molecular glue ternary structure prediction. *J Chem Inf Model* 2025. <https://doi.org/10.1021/acs.jcim.5c01860>
41. Rajan K, Zieslesny A, Steinbeck C. STOUT: SMILES to IUPAC names using neural machine translation. *J Cheminform* 2021;13:34. <https://doi.org/10.1186/s13321-021-00512-4>
42. Madhavi Sastry G, Adzhigirey M, Day T *et al.* Protein and ligand preparation: parameters, protocols, and influence on virtual screening enrichments. *J Comput Aided Mol Des* 2013;27:221–34. <https://doi.org/10.1007/s10822-013-9644-8>
43. Bouysset C, Fiorucci S. ProLIF: a library to encode molecular interactions as fingerprints. *J Cheminform* 2021;13:72. <https://doi.org/10.1186/s13321-021-00548-6>
44. Sehnal D, Bittrich S, Deshpande M *et al.* Mol* Viewer: modern web app for 3D visualization and analysis of large biomolecular structures. *Nucleic Acids Res* 2021;49:W431–7. <https://doi.org/10.1093/nar/gkab314>
45. Lipinski CA, Lombardo F, Dominy BW *et al.* Experimental and computational approaches to estimate solubility and permeability in drug discovery and development settings. *Adv Drug Deliv Rev* 2001;46:3–26. [https://doi.org/10.1016/S0169-409X\(00\)00129-0](https://doi.org/10.1016/S0169-409X(00)00129-0)
46. Roy N, Wyseure T, Lo I-C *et al.* Suppression of NRF2-dependent cancer growth by a covalent allosteric molecular glue. *bioRxiv*, <https://doi.org/10.1101/2024.10.04.616592>, 5 October 2024, preprint: not peer reviewed.
47. Coelho JPL, Yip MCJ, Olton K *et al.* The eRF1 degrader SRI-41315 acts as a molecular glue at the ribosomal decoding center. *Nat Chem Biol* 2024;20:877–84. <https://doi.org/10.1038/s41589-023-01521-0>
48. Palacino J, Swalley SE, Song C *et al.* SMN2 splice modulators enhance U1-pre-mRNA association and rescue SMA mice. *Nat Chem Biol* 2015;11:511–7. <https://doi.org/10.1038/nchembio.1837>
49. Wang J, Schultz PG, Johnson KA. Mechanistic studies of a small-molecule modulator of SMN2 splicing. *Proc Natl Acad Sci USA* 2018;115:E4604–12. <https://doi.org/10.1073/pnas.1800260115>